Modelling and Eigenanalysis of Sub-synchronous Oscillations Excited by Large Wind Power Plants

van Vledder, Cees; Rueda Torres, José ; Stefanov, Alex; Palensky, Peter; Anaya-Lara, Olimpo; Kruimer, Bas; Gonzalez-Longatt, Francisco

DOI
10.1109/MSCPES58582.2023.10123424

Publication date
2023

Document Version
Final published version

Published in
Proceedings of the 2023 11th Workshop on Modelling and Simulation of Cyber-Physical Energy Systems (MSCPES)

Citation (APA)
van Vledder, C., Rueda Torres, J., Stefanov, A., Palensky, P., Anaya-Lara, O., Kruimer, B., & Gonzalez-Longatt, F. (2023). Modelling and Eigenanalysis of Sub-synchronous Oscillations Excited by Large Wind Power Plants. In *Proceedings of the 2023 11th Workshop on Modelling and Simulation of Cyber-Physical Energy Systems (MSCPES)* (pp. 1-6). IEEE. https://doi.org/10.1109/MSCPES58582.2023.10123424

2023 11th Workshop on Modeling and Simulation of Cyber-Physical Energy Systems (MSCPES) | 979-8-3503-3682-5/23/$31.00 ©2023 IEEE | DOI: 10.1109/MSCPES58582.2023.10123424

Modelling and Eigenanalysis of Sub-synchronous Oscillations Excited by Large Wind Power Plants

Cees van Vledder, Jose Rueda Torres, Alex Stefanov, Peter Palensky
Intelligent Electrical Power Grids
Delft University of Technology
Delft, The Netherlands
[c.a.vanvledder, j.l.ruedatorres, a.i.stevanov,p.palensky]@tudelft.nl

Olimpo Anaya-Lara
Department of Electric Power Engineering
NTNU Norwegian University of Science and Technology
Trondheim, Norway
olimpo.anaya-lara@ntnu.no

Bas Kruimer
Digital Grid Operations
DNV Energy Systems
Arnhem, The Netherlands
bas.kruimer@dnv.com

Francisco Gonzalez-Longatt
Dept. of Engineering
DIgEnSysLab
University of Exeter
Exeter, UK
fglongatt@fglongatt.org

***Abstract*—The amount of power electronic interfaced generation (PEIG) is significantly proliferating in modern cyber-physical energy systems (CPESs). The limited capabilities (e.g. inertia, over-current) of PEIG, together with their location and technology-specific designed control systems, alter the dynamic properties of different types of stability phenomena, e.g. sub-synchronous oscillations (SSOs). A poorly damped SSO can emerge, within a sub-second time scale, through conflicting interactions between the controls of PEIG and the dynamic response of the surrounding electrical network. This paper focuses on the modelling and assessment of such interactions, with emphasis on the integration of large-size full converter (a.k.a. type-4) based wind power plants (WPPs). By combining different analysis tools, the implemented model supports sensitivity assessment of the occurrence and observability of a poorly damped SSO. State-space model based eigenanalysis is iteratively used to ascertain damping variability of a dominant SSO, excited by inappropriate controller settings of the WPP. Power spectral density (PSD) analysis is used to qualitatively estimate the degree of observability of the poorly damped SSO across different buses of a CEPS. Numerical tests are performed on a modified version of the IEEE-39 bus system by using DIgSILENT PowerFactory 2022 SP1. Suggestions are provided for the deployment of data generated from phasor measurement units (PMUs) in the monitoring and wide-area damping control of critical SSOs.**

***Index Terms*—Sub-synchronous oscillations, observability, phasor measurement units, control interaction, wide area monitoring and control**

I. Introduction

Wind power and other types of power electronic interfaced generation (PEIG) have an increasingly significant role in the electrical power system. PEIG modify the physical nature of dynamic phenomena or introduce new dynamics in modern cyber-physical energy systems (CPESs). One of these new dynamics are PEIG induced sub-synchronous oscillations (SSO), which have been usually attributed in fundamental research studies to sub-synchronous control interactions (SSCI) [1].

Undesirable SSOs were first observed in the '70 in an event in Mohave [2]. In this event, a compensated radial connection using a fixed series capacitor (FSC) on the line had a similar resonance frequency as the shaft of the generator. During the event, significant damage was caused to the shaft. Since this event, solutions have been proposed to prevent this kind of sub-synchronous resonance (SSR) [2].

A renewed interest in SSOs emerged when new sub-synchronous events occurred in the integration of large-scale wind power plants (WPP) in CPESs. The first known type of these new events was reported in 2009 in Texas in relation with the integration of type-3 wind turbine based WPPs [3]. In the subsequent years, other events were reported in the USA and China [4] [5]. The aforesaid events were caused by resonances excited by FSC, which were amplified by the so-called induction generator effect. Limiting the amount of compensation has been suggested as a possible effective mitigation measure [5]. Other alternative solutions are proposed in [6], such as SSR blocking filters or special protection to prevent topologies of CEPSs prone to SSR risk.

Another type of sub-synchronous phenomenon was then reported in China in 2015 [7]. In this case, no FSC were present nearby. This new event was categorized as SSCI [1]. In 2017 and 2019, other events were reported in China and the United Kingdom (UK), respectively [8] [9]. As a result of the SSO, the protection of WPPs and synchronous generation was activated during the event, leading to a significant loss of generation. In the event in UK this even resulted in a large load shedding. These were all events in which type-4 fully rated converters (FRC) played a role. Type-4 WPPs have a very similar layout as other PEIG, such as photovoltaics, battery energy storage systems and high-voltage direct-current (HVDC) links. As all types of PEIG will predominate and define the dynamic performances of future CPESs, it is crucial to understand both the mechanisms leading up to SSO and their propagation throughout physical electrical networks. Most SSOs have been attributed to the improper tuning of the control systems of the power electronic converters and weak grid conditions. [7] [8] [9] [10].

The previous paragraph shows a lot of effort has been put

979-8-3503-3682-5/23/$31.00 ©2023 IEEE

into investigating the factor leading up to SSO caused by type-4 WPPs. This includes control parameters on the current controller and phase locked loop (PLL) as well as network strength. Additionally, a different set of model and data driven tools is used in various published works. In [11], Fourier analysis is performed on sub-synchronous oscillations. By considering different ranges of control parameters for the inner control loop, the impact of a varying number of wind turbines in a WPP and network impedance on a sub-synchronous oscillatory frequency are investigated. In [12], the influence of the inner control loop parameters and additional filters is looked into. In these studies, linearized state-space model and signal record based eigenanalysis supported by experimental time-domain simulations are suggested as suitable assessment tools. The main emphasis of the assessment has been on possible changes of oscillatory frequencies and damping ratios. Furthermore, the influence of the PLL is receiving significant attention in recent research works. The PLL is used to track the rotating frame of the fundamental frequency of the system. In [13], the influence of the PLL control parameters is investigated by performing time-domain simulations and eigenanalysis in selected operating conditions. [7] presents an analytical derivation on the amplification of a small-size disturbance through the PLL. From this analytical assessment, a criterium is suggested to determine when a disturbance could be amplified.

The aforesaid works are focused to critical factors leading to unstable sub-synchronous oscillations. This leaves a gap in knowledge in propagation of SSO in a high voltage transmission network. Since bus voltages and power flows are not state variables in a linear state-space model, it is challenging to determine the observability analytically. In [14], an analytical derivation is given on voltage oscillations using a network model and mode shapes of the state variable of the rotor angles of the synchronous generators. Since type-4 WPP induced SSOs are not caused by rotor angle oscillations, this method cannot be used. However, a similar fundamental study for PEIG based power systems could provide great insight into the propagation and observability of SSOs.

In view of the above, this paper aims at qualitatively shedding light on the observability of SSO induced by large-size type-4 WPPs integraged in CPESs. Also the potential of the use of PMU data for the detection and damping control systems is shown. This paves the way for future work on analytical data driven methods to determine the observability of a poorly damped SSO. For instance, this can be used to determine the observability for Phasor Measurement Unit (PMU) based applications of critical SSO modes caused by PEIG. Supplementary wide-area monitoring and control (WAMC) systems, which yield new forms of supplementary damping support, could also be developed, taking PMU signals into account.

Section II of the paper describes the adopted methodological aspects. This involves the use of a linear dynamic CPESs model for state-space based eigenanalysis. This is used to determine the oscillatory mode sensitivity to the control parameters of the inner control loop of the WPP. This is followed by time-domain simulations on an identified poorly damped mode and its power spectral density (PSD) analysis. Section III analyses the results of the time-domain simulations by using Fourier analysis. These results are represented in the context of the network topology in order to visualize the variable levels of observability of the SSO. In section IV, concluding reflections and an outlook for future work are concisely given.

II. Methodology

To analyse the behaviour of SSOs in a transmission network, an operating condition is created in which a WPP excites a poorly damped SSO mode. A modified IEEE-39 bus system simulated in DIgSILENT PowerFactory 2022 SP1 is chosen. The 39 bus system originally has 10 synchronous generators, 19 loads and no PEIG [15]. Previous works show that weak nodes are more prone to sub-synchronous oscillations [11], [12]. Therefore, a WPP model is connected to bus 12. At the same time, transformer 11-12 is disconnected, which is one of the two transformers connecting this bus. The adopted WPP model corresponds with the DIgSILENT FullyRated-Conv WTG 6.0MW template [16]. The model only represents only the grid side converters of the WPP. The model uses 175 aggregated wind turbines resulting in a WPP with a rated output of 1050 MW.

A linearized state-space model enabling eigenanalysis is used to analytically evaluate the resulting sub-synchronous oscillatory behaviour. This is supplemented by PSD analysis of selected signals generated by time-domain simulations. The effects on the bus voltage phasors are analysed. This is separated in terms of voltage magnitude V_i and voltage angle θ_i of each bus i. A schematic overview of the adopted methods is shown in Fig. 1.

A. Linear Dynamic Model for Eigenanalysis

By using the state-space modelling functionality of PowerFactory, the dynamic system is linearized around the considered equilibrium point. The linear model is defined by (1).

$$\frac{d\mathbf{x}}{dt} = \mathbf{A}\mathbf{x} \tag{1}$$

where $\mathbf{x}$ is a vector containing the 180 state variables of the dynamic model. These state variables are both physical quantities, such as rotor speeds of the synchronous generators, as well as controller signals. $\mathbf{A}$ is a square matrix which represents the state-space model dynamic behaviour. From the state space model, eigenvalues and right eigenvectors are obtained by using the `eig` function of MATLAB R2021b. The calculation is represented by (2).

$$\mathbf{A}\boldsymbol{\phi}_j = \lambda_j \boldsymbol{\phi}_j \tag{2}$$

where $\boldsymbol{\phi}_j$ is the right eigenvector associated with the j-th eigenvalue λ_j of corresponding mode j. λ_j is related to the frequency and damping of a system oscillation mode by the imaginary and real part of the eigenvalue respectively. $\boldsymbol{\phi}_j$ represents the amplitude and phase of each state variable using complex values for mode j. There are as many modes

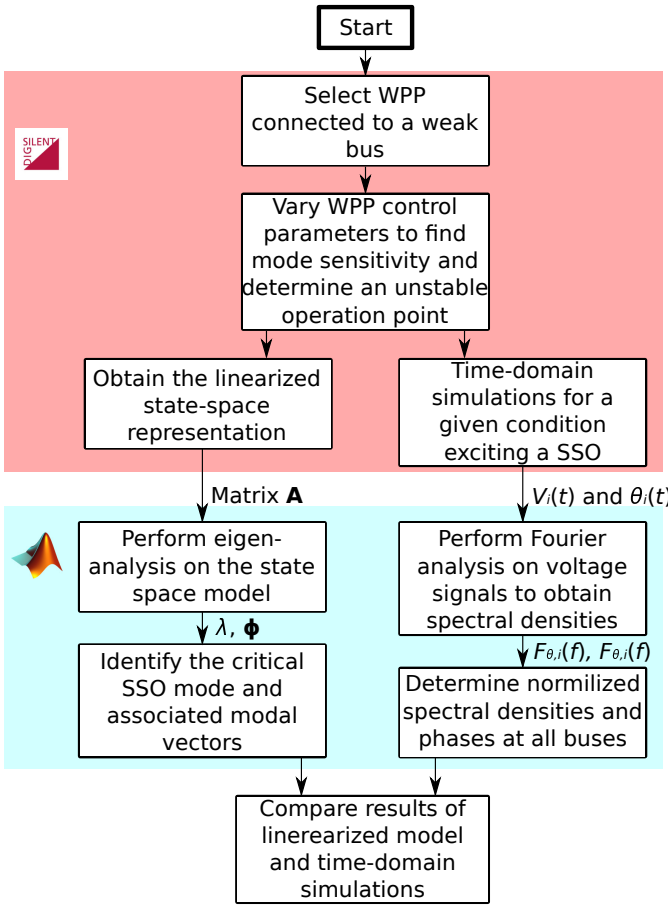

Fig. 1. Overview of methodology used in a complementary model based eigenanalysis and time-domain simulation based PSD.

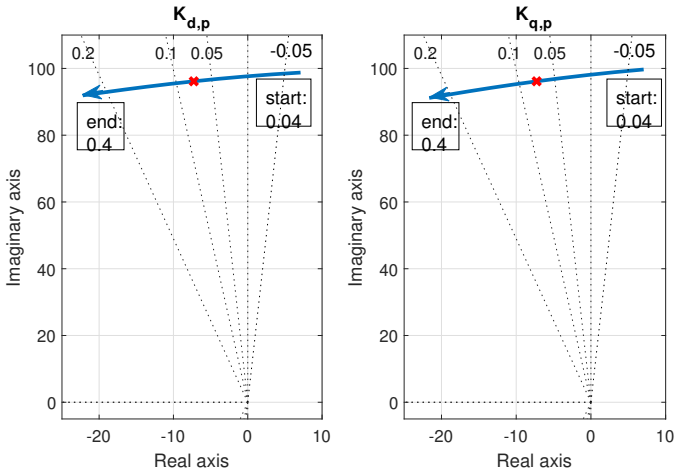

Fig. 2. Parametric sensitivity of the eigenvalue of the sub-synchronous mode to proportional gains of the inner control loop. The red point indicates the eigenvalue for the reference value of the control parameter. The gains are varied between 0.04 and 0.4. The dashed lines indicate the damping ratio.

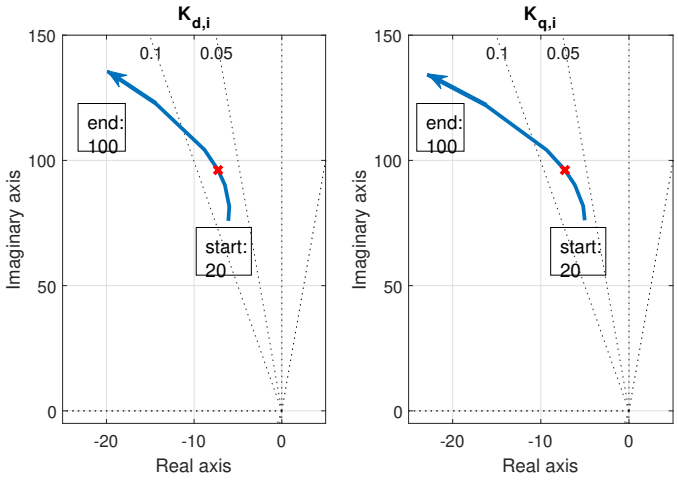

Fig. 3. Parametric sensitivity of the eigenvalue of the sub-synchronous mode to integrational gains of the inner control loop. The red point indicates the eigenvalue for the reference value of the control parameter. The gains are varied between 20 and 100. The dashed lines indicate the damping ratio.

and thus eigenvalues and eigenvectors as the number of state variables in the dynamic system. Because of these properties, the eigenvalues can be used to identify and trace a critical sub-synchronous oscillation in the complex plane.

B. Control Parameter Sensitivity

The WPP power output is set to 50% of the rated output. The control system of the WPP model consists of an outer and inner control loop [16]. Previous work has shown that the inner control loop and the PLL mainly influence the sub-synchronous behaviour due to their faster dynamics [7]. The inner control loop is connected to a PLL, which uses a PI controller, to track the voltage angle at the interconnection bus. This angle is used to transform the current output to a dq-frame. This allows for separate PI control of the d- and q-currents. Improper tuning of these control parameters can lead to an increased risk of a SSO [17].

The sensitivities to the control parameters of the inner control loop are investigated. Start values consider reference values of gains assumed as $K_{PLL,p}$ = 3, $K_{PLL,i}$ = 100, $K_{d,p}$=$K_{q,p}$=0.2, and integral gains assumed as $K_{d,i}$=$K_{q,i}$=40, which are based on the standard values of the WTG template in PowerFactroy.

For the analysis, one of the inner control loop parameters is varied at a time, while other parameters are kept constant. In this way, a single parametric influence on the sub-synchronous oscillatory mode is traced. The results of the parametric sensitivity are shown in Fig. 2 and 3. In each figure, the eigenvalue defining the sub-synchronous oscillatory mode λ_{SSO} in the start reference values of the parameters is highlighted with red. Similar to results from literature, these results show that the proportional gains mainly influence the damping of the sub-synchronous oscillatory mode [10]. The integral gains have also a strong influence on the frequency of sub-synchronous mode.

In order to perform time-domain simulation of an undesirable sub-synchronous oscillatory behaviour, an unstable operating condition is selected. The proportional gains are lowered to

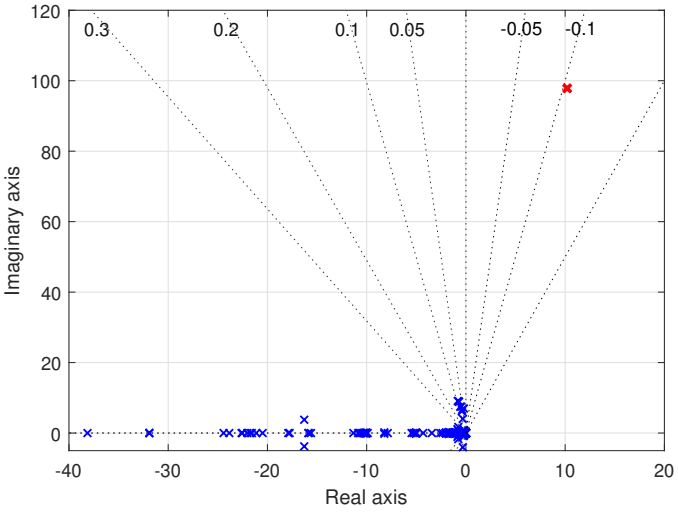

Fig. 4. Eigenvalues of the modified IEEE-39 bus system, which includes a large-size WPP at bus 12. The red eigenvalue corresponds to the sub-synchronous mode.

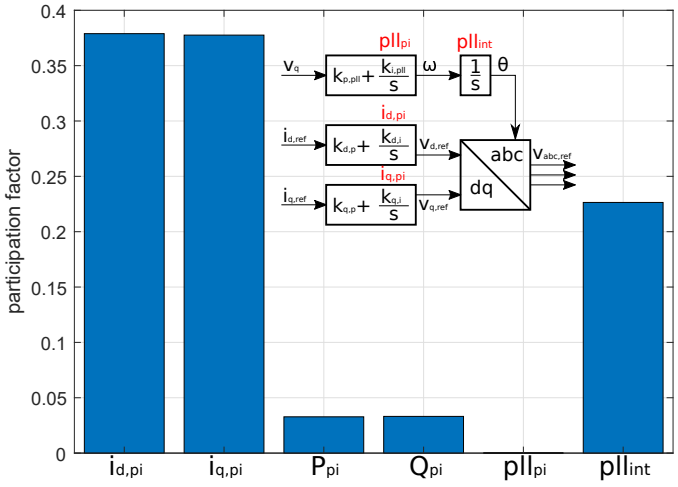

Fig. 5. Participation factors associated with the unstable sub-synchronous oscillatory. A small section of the current controller and the PLL of the WPP are depicted as well. Each red character denotes the state variable of the block.

$K_{d,p} = K_{q,p} = 0.1$, while the other control parameters are kept at their reference settings mentioned previously. This set of control parameters and under weak network operation yields an unstable oscillatory mode, which is located in the right-hand plane. Fig. 4 shows all eigenvalues of the system. The sub-synchronous mode is clearly distinguished from the other modes by its higher frequency. The eigenvalue of the sub-synchronous oscillatory mode is $\lambda_{SSO} = 10.3 \pm j97.8$. The other modes correspond to known low-frequency electro-mechanic oscillatory modes of the IEEE-39 bus system [15]. The participation factors are calculated to corroborate if the identified sub-synchronous oscillatory mode can be associated with the added WPP. Similarly to the definition of right eigenvector $\boldsymbol{\phi}$, a left eigenvector is defined by (3).

$$\boldsymbol{\psi}_k \mathbf{A} = \boldsymbol{\psi}_k \kappa_k \tag{3}$$

where $\boldsymbol{\psi}_k$ is the k-th left eigenvector and κ_k is an eigenvalue related value. The elements of the left and right eigenvector are used to calculate the participation factors.

$$p_{j,k} = \boldsymbol{\phi}_{k,j} \boldsymbol{\psi}_{j,k} \tag{4}$$

where $p_{j,k}$ represents the participation of the k-th state variable in the j-th mode. The participation factors are normalised (dimensionless) values.

The most significant participation factors are shown in Fig. 5. All other state variables have an insignificant participation factor. The participation factors show that the controller of the WPP plant has a significant participation in the sub-synchronous oscillatory mode. Especially, the inner control loop and the PLL have a significant participation. No other state variables of other system components have a significant participation in the sub-synchronous oscillatory mode. This confirms that this mode is caused by SSCI of the WPP.

C. Time-domain simulations and PSD analysis

In order to qualitatively ascertain the observability of the SSO, PowerFactory 2022 SP1 is used to perform root-mean-square time-domain simulations. The simulations are performed over 10 s with an integration step of 0.1 ms. During each simulation, the voltage phasors on all buses are stored for analysis. The voltage magnitude $V_i(t)$ and voltage angle $\theta_i(t)$ of all buses are shown in Fig. 6 for the first 4 seconds of the simulation. These quantities are chosen for the analysis because they resemble signal records that can eventually be acquired by using PMU devices. During the first 2 seconds, the system is stable. From the equilibrium initial conditions, it takes about 2 seconds before the instability becomes visible. No event is simulated to trigger this oscillation, which is expected due to the identified unstable oscillatory mode of the system. Between 2-3 seconds, a growing oscillation is visible. After 3 seconds, a sustained oscillation is observed. This oscillation stabilizes until the end of the simulation period, which is not fully shown.

The results of the sustained oscillation between 4-10 seconds are used to perform a Fast Fourier Transform (FFT) in MATLAB R2021b. This results in a PSD of the oscillations $\Delta V_i(f)$ and $\Delta\theta_i(f)$. The obtained PSDs are shown in Fig. 7. A high peak is visible at 16.9 Hz, representing the sub-synchronous frequency f_{SSO}. This frequency is close to the frequency given by the eigenvalue frequency imag(λ_{SSO}) of 15.6 Hz, shown in Fig. 4.

For further analysis, the PSD at the sub-synchronous frequency are normalized to the PSD of bus 12, where the WPP is connected. This results in the values of $F_{V,i}$ and $F_{\theta,i}$ for each bus i in the system. (5) and (6) are used to calculate these values.

$$F_{V,i} = \frac{\Delta V_i(f_{SSO})}{\overline{\Delta V}_{WPP}(f_{SSO})} \tag{5}$$

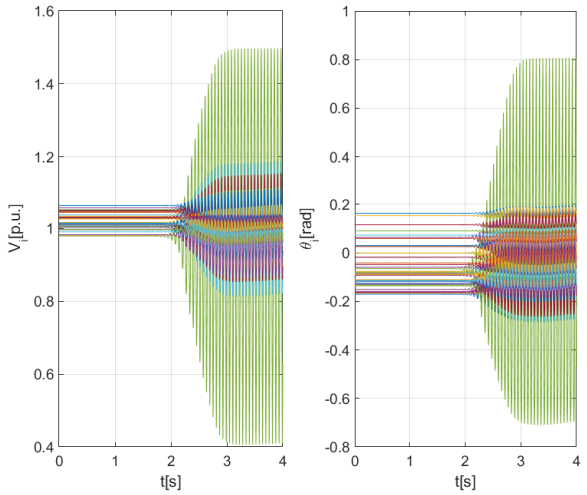

Fig. 6. Bus voltages of the modified IEEE-39 bus system, illustrating the excitation of a poorly damped SSO. The voltage magnitudes $V_i(t)$ are shown on the left. The voltage angles $\theta_i(t)$ are shown on the right. The largest oscillations are on bus 12.

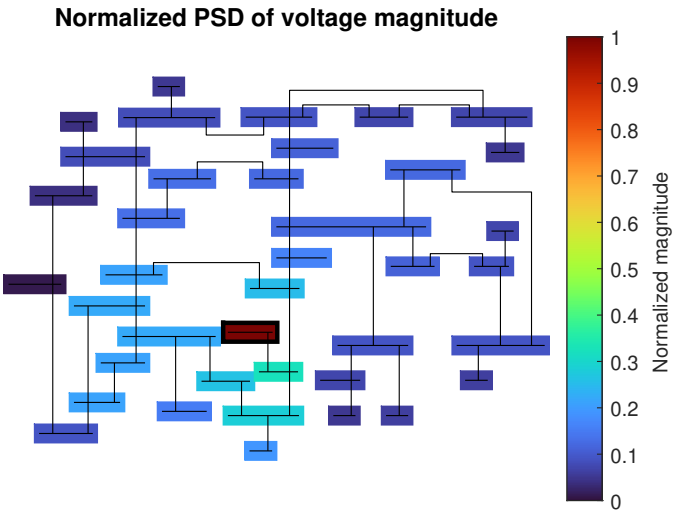

Fig. 8. Magnitude of the PSDs of the voltage magnitude oscillation at the sub-synchronous frequency $F_{V,i}$ in the modified IEEE-39 bus system. Bus 12 is indicated in the black square.

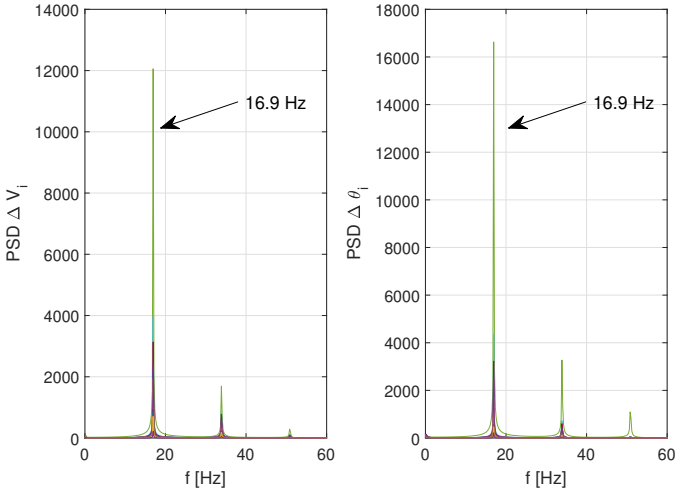

Fig. 7. PSD of the sustained SSOs. The computed PSDs for bus voltage magnitudes are shown on the left. The computed PSDs for bus voltage angle are shown on the right.

$$F_{\theta,i} = \frac{\Delta\theta_i(f_{SSO})}{\overline{\Delta\theta}_{WPP}(f_{SSO})} \tag{6}$$

The PSD results have a magnitude and phase components which can be simultaneously analyzed. The phase represents the lag or lead of oscillation relative to other buses. In (5) and (6) the phases of the normalized values are set relative to the results of bus 12 by using the conjugate value in the denominator.

III. Analysis of Results

The magnitudes of the normalized values of $F_{V,i}$ are shown in Fig. 8. The results are represented in the context of the network topology. Bus 12, indicated in red, is where the WPP is connected to. Other buses have a significantly lower PSD, which corroborates the fact that the SSO is a local phenomenon.

In Fig. 9, the values of $F_{\theta,i}$ are shown. These results generally show a similar result compared with $F_{V,i}$ where the strongest PSD is close to the WPP. However, the decay in PSD moving away from the WPP is stronger for the voltage angle oscillation, indicated by the darker blue colors.

To understand the sub-synchronous behaviour, a perturbation for sub-synchronous current injection i_{SSO} is introduced. As the control parameters of the WPP are not properly set, this change is not damped. As the injected current has a sub-synchronous frequency, it oscillates relative to the voltage. This causes a perturbation for active power output and reactive power output. This is refered to as P_{SSO} and Q_{SSO} respectively. As voltage phasor angles are associated with active power flows and voltage magnitude with reactive power flows, this suggests that Q_{SSO} flows penetrate the network more prominently than P_{SSO}. The penetration of these oscillations are limited by the resistance in the lines which dissipates these oscillations. In Fig. 10, the phases of the normalized values $F_{V,i}$ and $F_{\theta,i}$ are shown in the network topology. These phase shifts are related to a lag or lead of the SSO in $V(t)_i$ and $\theta(t)_i$. The results show a significant phase shift in a different parts of the network for the SSO. The SSO created in this scenario only has one source, which makes it fundamentally different from other low-frequency oscillation modes (e.g. intra area modes of synchronous generators). The phase differences at different buses are only the results of the impedance and inherent damping throughout the network. The phases of $\angle F_{V,i}$ lag to the oscillation at the WPP. The phases of the voltage angle oscillations $\angle F_{\theta,i}$ show a more complex response. Moving away from bus 12, the oscillations leads.

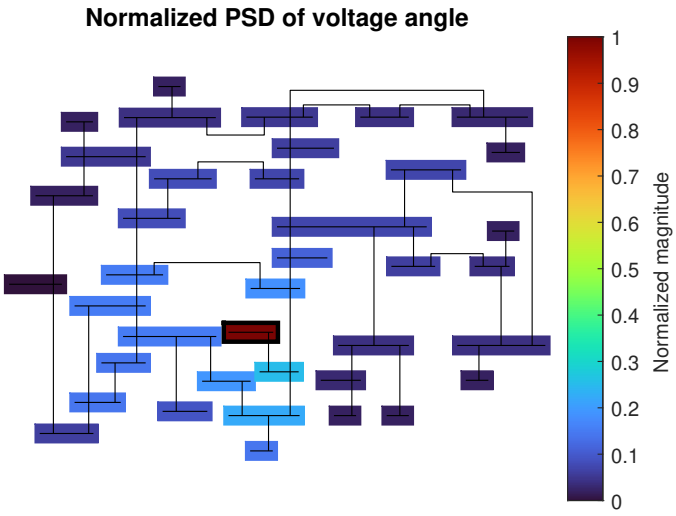

Fig. 9. Magnitude of the PSDs of the voltage angle oscillation at the sub-synchronous frequency $F_{\theta,i}$ in the modified IEEE-39 bus system. Bus 12 is indicated in the black square.

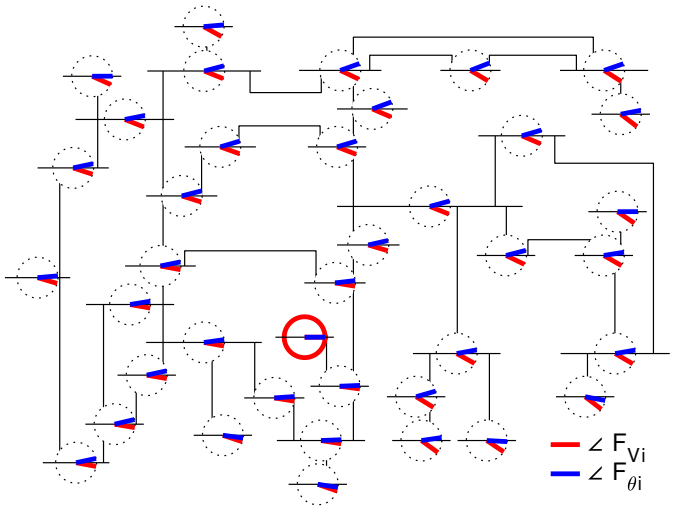

Fig. 10. Phases of the PSD value $\angle F_{V,i}$ (red) and $\angle F_{\theta,i}$ (blue) at the sub-synchronous frequency f_{SSO} in the modified IEEE-39 bus system. The red circle indicates the connection of the WPP.

However, at buses where a synchronous generator is connected to the system, the oscillation lags to the connected bus. This is caused by the interaction of damping in active power of the synchronous generators. This further points out a difference in active power oscillations and reactive power oscillations of the SSO. The phase difference throughout the network are slightly influenced by the distance from the source. This contrasts with the oscillation magnitude. These findings are essential to identify the source of a SSCI in a transmission network.

IV. Conclusions

In this paper, SSOs are simulated in a modified IEEE-39 bus system, integrating a WPP. Small-signal analysis is used to find the sensitivity of the sub-synchronous mode to the inner control loop parameters. Using these results, an unstable operation point is determined. State-space model based eigen-analysis is performed to show SSCI due to type-4 WPP as the source of the SSO. A time-domain simulation corroborates the excitation of the unstable SSO. Time simulation is analysed further to find qualitative results on the propagation of the SSO in magnitude and phase throughout the network. The findings from the qualitatively analysis can be used to define and test a multi-parameter analytical method to determine the observability of SSO induced by PEIG. Such an analytical method for the observability of SSO could yield analogous analytical observability metrics like those presented in [14].

References

[1] Sewdien, V., Wang, X., Torres, J. R. and Van Der Meijden, M., "Critical Review of Mitigation Solutions for SSO in Modern Transmission Grids", July 2020.

[2] Hodges, D. A., Bowler, C. E. and Jackson, R. L. "Results of Sub-synchronous Resonance Test at Mohave", IEEE Transactions on Power Apparatus and Systems, vol. 94, pp. 1878–1889, 1975.

[3] Adams, J., Carter, C. and Huang, S. H., "ERCOT Experience with Sub-Synchronous Control Interaction and Proposed Remediation", Proceedings of the IEEE Power Engineering Society Transmission and Distribution Conference, 2012.

[4] Yunhong, L., Hui, L., Xiaowei, C., Jing, H. and Ul I, Y., "Impact of PMSG on SSR of DFIGs Connected to Series-Compensated Lines Based on the Impedance Characteristics", The Journal of Engineering, 2017.

[5] Narendra, K. et al., "New Microprocessor Based Relay to Monitor and Protect Power Systems against Sub-Harmonics", 2011 IEEE Electrical Power and Energy Conference, EPEC 2011, pp. 438–443, 2011.

[6] NERC, "Lesson Learned - Sub-Synchronous Interaction between Series-Compensated Transmission Lines and Generation", tech. rep., Atlanta, USA, July 2011.

[7] Xu, Y. and Cao, Y., "Sub-Synchronous Oscillation in PMSGs Based Wind Farms Caused by Amplification Effect of GSC Controller and PLL to Harmonics", IET Renewable Power Generation, vol. 12, pp. 844–850, 2018.

[8] Xu, Y., Zhao, S., Cao, Y. and Sun, K., "Understanding Subsynchronous Oscillations in DFIG-Based Wind Farms Without Series Compensation", IEEE Access, vol. 7, pp. 107201–107210, 2019.

[9] National Grid ESO, "Technical Report on the Events of 9 August 2019", technical report, 2019.

[10] Liu, H., Xie, X., He, J., Xu, T., Yu, Z., Wang C. and Zhang, C., "Subsynchronous Interaction Between Direct-Drive PMSG Based Wind Farms and Weak AC Networks", IEEE Transactions on Power Systems, vol. 32, pp. 4708–4720, November 2017.

[11] Yan, G., Wan, Q., Jia, Q. and Liu, J., "Analysis of SSO Characteristics of D-PMSGs Based Wind Farm under Weak AC System", 2nd IEEE Conference on Energy Internet and Energy System Integration, EI2 2018 - Proceedings, December 2018.

[12] Adib, A., Mirafzal, B., Wang, X. and Blaabjerg, R., "On Stability of Voltage Source Inverters in Weak Grids", IEEE Access, vol. 6, pp. 4427–4439, December 2017.

[13] Li, Y., Fan, L. and Miao, Z., "Wind in Weak Grids: Low-Frequency Oscillations, Subsynchronous Oscillations, and Torsional Interactions", IEEE Transactions on Power Systems, vol. 35, pp. 109–118, January 2020.

[14] Vanfretti, L. and Chow, J. H., "Analysis of Power System Oscillations for Developing Synchrophasor Data Applications", 2010 IREP Symposium Bulk Power System Dynamics and Control-VIII, IREP, pp. 1-17, IEEE, 2010.

[15] DIgSILENT GmbH, "39 Bus New England System", DIgSILENT PowerFactory GmbH, tech. rep., Gomaringen, Germany, 2020.

[16] DIgSILENT GmbH, "Technical Reference DIgSILENT Fully Rated Converter Wind Turbine Templates", DIgSILENT PowerFactory GmbH, tech. rep., Gomaringen, Germany, 2022.

[17] Du, W., Wang, X. and Wang, H., "Sub-Synchronous Interactions Caused by the PLL in the Grid-Connected PMSG for the Wind Power Generation", International Journal of Electrical Power and Energy Systems vol. 98, pp. 331–341, June 2018.